



ISSN NO. 2320-5407

Journal Homepage: [-www.journalijar.com](http://www.journalijar.com)

INTERNATIONAL JOURNAL OF ADVANCED RESEARCH (IJAR)

Article DOI: 10.21474/IJAR01/15878
DOI URL: <http://dx.doi.org/10.21474/IJAR01/15878>



INTERNATIONAL JOURNAL OF
ADVANCED RESEARCH (IJAR)
ISSN 2320-5407
Journal Homepage: <http://www.journalijar.com>
Journal DOI: 10.21474/IJAR01

RESEARCH ARTICLE

STUDY OF THE THERMOCHEMICAL AND MECHANICAL PROPERTIES OF LATERITE BRICKS STABILISED WITH CEMENTS.

B. Kossi Imbga^{1,2}, Séckou Bodian³, Pape M. Toure³, Younouss Dieye³ and Vincent Sambou³

1. Laboratoire de Recherche en Météorologie et l'Espace (LAREME); Université Norbert ZONGO.
2. Laboratoire d'Energie Thermique Renouvelable (LETRE), Université de OUAGA I Joseph KI-ZERBO.
3. Laboratoire Eau, Energie, Environnement et Procédés Industriels (LE3PI); Ecole Supérieure Polytechnique (ESP) de DAKAR Université Cheikh Anta Diop (UCAD)-Sénégal.

Manuscript Info

Manuscript History

Received: 15 October 2022

Final Accepted: 18 November 2022

Published: December 2022

Key words:-

Thermal conductivity, Thermal Effusivity, Compressive Strength, Asymmetric Hot Plane, Laterite Bricks

Abstract

In this work, we characterised the thermophysical parameters of Thick laterite as a function of water content and also as a function of the cement content in the mix. For laterite with a diameter less than or equal to 1.25 mm, the thermal conductivity is 0.388 W/m.K for a water content close to 0%, this thermal conductivity increases to 87.37% for a water content of 3.46%. Laterite without cement has a strength of 2.309 MPa, this strength increases by 4.80 %, 13.16 %, 18.45 % and 47.82 % respectively when 4 %, 6 %, 8 % and 10 % cement is added to the laterite. The flexural strength changes with the cement content of the mix, from 0.24 MPa for simple laterite to 0.510 MPa when 10% cement is added to the laterite health.

Copy Right, IJAR, 2022, All rights reserved.

Introduction:-

The construction industry is responsible for approximately 9 –10% of global CO₂ emissions, mainly due to cement production [1]. In this context, the tendency is to encourage the use of environmentally friendly construction materials that collaborate in reducing energy consumption in buildings, which is considered the most promising way to mitigate climate change. Global energy consumption in buildings accounts for approximately 40% of total energy consumption and is responsible for 25% of total carbon dioxide (CO₂) emissions [2]. In sub-Saharan Africa, this consumption is in the order of 50-70% [3]. This high energy consumption is due to the fact that concrete remains the main building material used, as it is a conductive material, its use in buildings always leads to the use of fans and air conditioners for thermal comfort. The life cycle analysis of this material shows that it has a high grey energy and environmental impact. Therefore, the use of alternative materials to concrete with low environmental impact becomes a necessity. This explains the fact that local building materials, especially mud bricks, have been gaining interest because they are a low grey energy material with low environmental impact. Several studies have been carried out to determine the mechanical, thermal and chemical properties of local building materials. Among them, Toure et al (2019) [4] showed that the use of earth bricks with high volumetric thermal capacity reduces energy consumption in buildings. Recently Kowa Eric et al (2021) [5] aimed to determine the thermal and mechanical properties of an eco-material "poto-poto" in Cameroon associated with bamboo fibres. The asymmetric hot plane method was used to characterise the thermal properties. The thermal conductivity of this material without bamboo fibre is 1.15 W/m.K, it increases to 0.95 W/m.K if 2% fibre is added to this material. The results obtained indicate that adding 6% fibre to this material provides good thermal insulation and energy savings. Alternative materials, such as cement-stabilised earth blocks (CSEB), offer new possibilities for environmentally friendly envelopes. Earth materials used for masonry are readily available,

Corresponding Author:- Séckou Bodian

Address:- Laboratoire d'Energie Thermique Renouvelable (LETRE), Université de OUAGA I Joseph KI-ZERBO.

abundant in nature, and their use minimises environmental impacts and improves the thermal performance of bricks. Moisture and cement content must be optimised for each type of soil in order to produce BTC. In the same vein, Adriana Belén Costantini Romero [6] was in charge of evaluating the influence of moisture and cement content in soil-cement mixtures. The results show that compacted silt with a very low sand fraction and a cement content between 3% and 9% has a low thermal conductivity and a low capacity to exchange heat with the environment when the moisture content is low enough. Younoussa Millogo et al (2012) [7] studied the physical and mechanical properties of compressed adobe blocks reinforced with Hibiscus Sabdarifa fibres. They find that with 0.02% to 0.06% by mass of 30 cm long fibres, the pores in the compressed adobe blocks are reduced and its mechanical properties are improved. However, the addition of 0.08% by mass of 60 mm long fibres has negative effects on the compressive strength. The use of local materials in construction is based on the knowledge of their thermophysical properties. Several studies have been conducted and published on local building materials. Laaroussi et al [8, 9] studied the thermophysical properties of clay stabilised with esparto fibres using the asymmetric hot plane method, the average conductivity obtained is 0.346 W/m.K. Pierre Meukam [10] studied the thermal and mechanical properties of laterite stabilised with cement for building thermal insulation. The box method was used to estimate the thermal conductivity of the laterite plus 8% cement mixture. The average value of thermal conductivity obtained by Meukam is 0.95 W/m.K. Imbga et al [11], aimed to determine the thermal and mechanical performance of laterite stabilized with cowpea pod for building thermal insulation. The thermal conductivities of laterite blocks associated with rates ranging from 0% to 16% with a 4% pitch of néré pod were determined. It was found that the thermal conductivity decreases as the percentage of dwarf pods increases. But it stabilizes from 14 to 16% with a corresponding value of 0.427 W/m.K. Jean Claude Damfeu et al. [12], characterized laterite of 1 mm diameter using the asymmetric hot plane method, the estimated thermal conductivity is 0.254 W/m.K and the estimated thermal effusivity is 534 J/K.m².s^{1/2}. The heat capacity and density of laterite stabilised with different millet pod contents and as a function of water content, were studied by H. Bal et al. [13], it was found that the estimated heat capacity of laterite by mass is 895 J/K.kg and that the thermal conductivity of the laterite and millet pod mixture increases as a function of water content. The effect of neem (*Azadirachta Indica*) fibres on the mechanical, thermal and durability properties of adobe bricks was studied by Colbert Babé et al. [14]. The hot plane method was used to characterise the materials, the conductivity of the adobe without fibre is 0.97 W/m.K. Séckou Bodian et al. (2018) [15] characterised the fired clay and unfired clay associated with various percentage rates of laterite collected from the Thicky site. The thermophysical characterisation method used was the asymmetric hot plane method. The results indicate that the thermal conductivity of the clay associated with 30% laterite has a thermal conductivity of 0.64 W/m.K, this value is reduced by 46.87% when the same formulation is fired. The thermal effusivity is 1280 J/K.m².s^{1/2} for the mud brick with 30% laterite. This value is reduced by 37.18% when the same brick with 30% laterite is fired. Touré et al. [16], stabilised laterite associated with 10% cement, the thermal conductivity obtained for this mixture is 0.81 W/m.K. Our objective is to characterise these new materials obtained from the laterite/cement mixture and lime. We therefore used the asymmetric lime plane method in transient regime to determine the thermal effusivity and the hot plane method in steady regime to determine the thermal conductivity.

Materials and Methods:-

Laterite

The laterite we used comes from the Thicky quarry in the Thies region of Senegal. It is composed of grains with a diameter of 1 mm or less. The Atterberg limits and grain size, of the laterite were studied by Séckou Bodian et al. [15]. The results obtained are: $W_p = 21.9\%$; $W_L = 38\%$; $I_p = 16.1\%$. The fineness modulus is 2.476.

The value of the plasticity index (I_p) shows that Thicky laterite is moderately plastic. The bricks manufactured for the thermal tests have a size of 10 x 10 x 2.5 cm³.

Presentation of the site

The soil of Senegal contains a large number of laterite deposits. Laterite is mainly used for road construction.

Despite the great potential of laterite extraction, it is less and less used in construction. The study was carried out on laterite collected from the Thicky quarry. Thicky is located in the Thiès region, in western Senegal at 14°50' N, 17°06' W. The geographical map is shown in Figure 1.

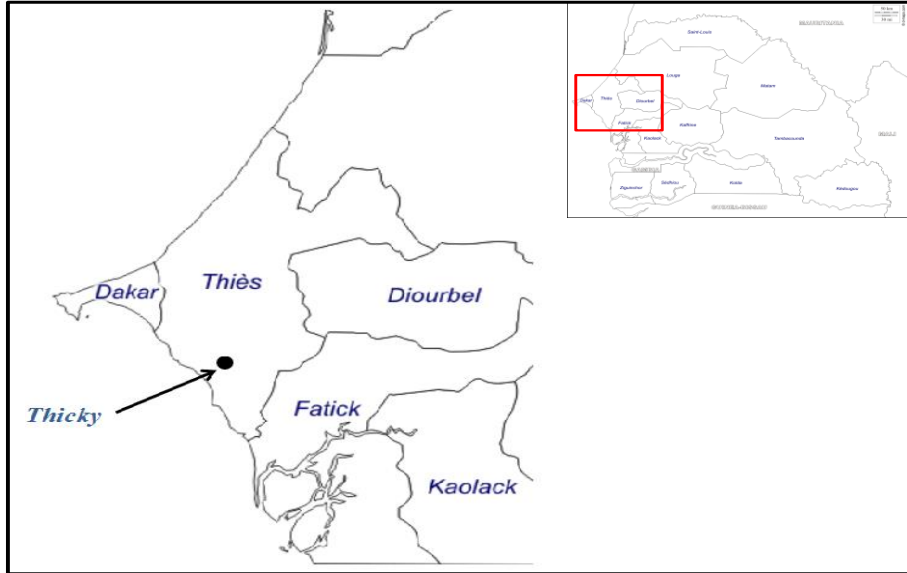


Figure 1: Location of Thicky in the Thiès region of Senegal [15].

Particle size analysis

The particle size analysis presents the percentage distribution of solid particles according to their size. The particle size distribution of laterite is shown in Figure 2. The result indicates that our material is mainly composed of sand (80%) and gravel (20%). The percentage of fines is 2.08% which shows that we are dealing with a preferential sand.

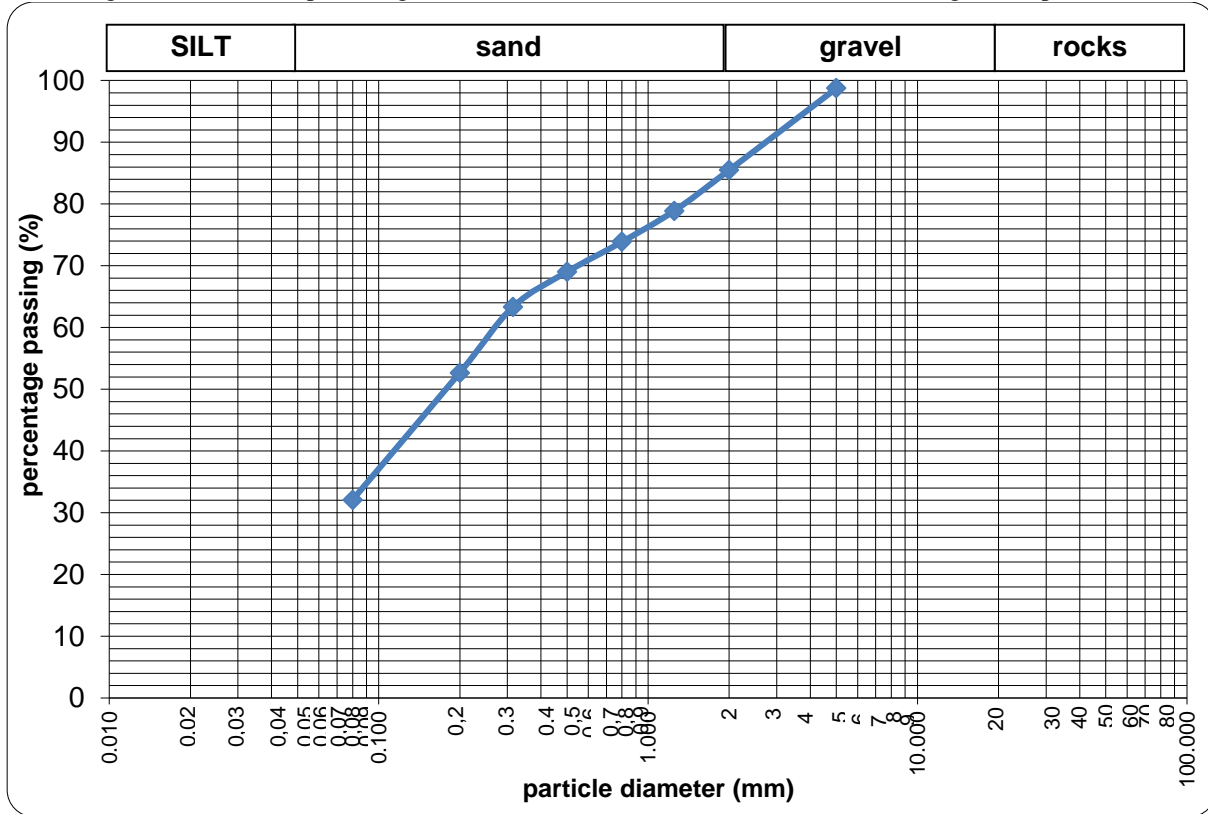


Figure 2: Particle size distribution of laterite

Method of measuring the chemical, thermal and mechanical characteristics of the different formulations**Chemical method****X-ray diffraction (XRD)**

The mineralogical composition of the samples was determined by the X-ray diffraction technique. This technique allows the identification of the different crystallised mineral phases present in the sample.

Infrared spectroscopy (IR)

Infrared spectrometry is one of the most widely used methods for the characterisation and identification of organic molecules. It is used to determine the functional groups present in the material. It is a fast and sensitive method for characterising most existing molecules.

Infrared spectrometry measures the decrease in intensity of radiation passing through a sample as a function of wavelength. The infrared spectroscopy method requires the use of an infrared-transparent medium such as potassium bromide (KBr). The method involves grinding a few milligrams (0.5 to 1 mg) of the sample in the presence of dry KBr powder in an agate mortar. The mixture is then compressed in a hydraulic press.

Chemical analysis of raw materials

Elemental chemical analysis consists of measuring the various chemical elements that make up the sample in atomic form.

The elemental chemical analysis of our raw materials was obtained by ICP-AES (Inductively Coupled Plasma Atomic Emission Spectrometry). Nitric (HNO_3) (2 ml) and hydrofluoric (HF) acids (6 ml) were used for wet solution in a volume of 100 ml. The results were obtained at a pressure of 60 bar with a step of 0.8 bar/second, at a temperature of 240°C, with a power of 900 W, a ramp of 20 min and a step of 30 min.

Differential Thermal Analysis (DTA)

Differential thermal analysis is based on the thermal reactions that occur when a compound is heated. The curve obtained highlights the loss of water (endothermic reactions), but also recrystallisations, recombinations (exothermic reactions) and the oxidation of organic matter. DTA is a technique that measures the difference in temperature between a sample and a reference "thermally inert material" as a function of time or temperature when subjected to a temperature program in a controlled atmosphere.

SEM microscopic observations

The Scanning Electron Microscope (SEM) allows the surface topography of a sample to be observed by scanning its surface with an electron beam and collecting the image formed. In the case of our samples, the clay powder was deposited on a carbonaceous pellet. This wafer is then metallised by coating it with a thin layer of metal using platinum sputtering to make it conductive. Once metallised, the sample is introduced into the SEM chamber for analysis.

Thermal method

We used the asymmetrical hot plane method, available at the Applied Energetics Laboratory (LEA) of the Higher Polytechnic School of Dakar, to determine the thermal properties of laterite, to which we progressively added a rate of 4%, 6%, 8%, 10% and 12% of mass of cement in order to observe the evolution of the thermal and mechanical properties of these mixes.

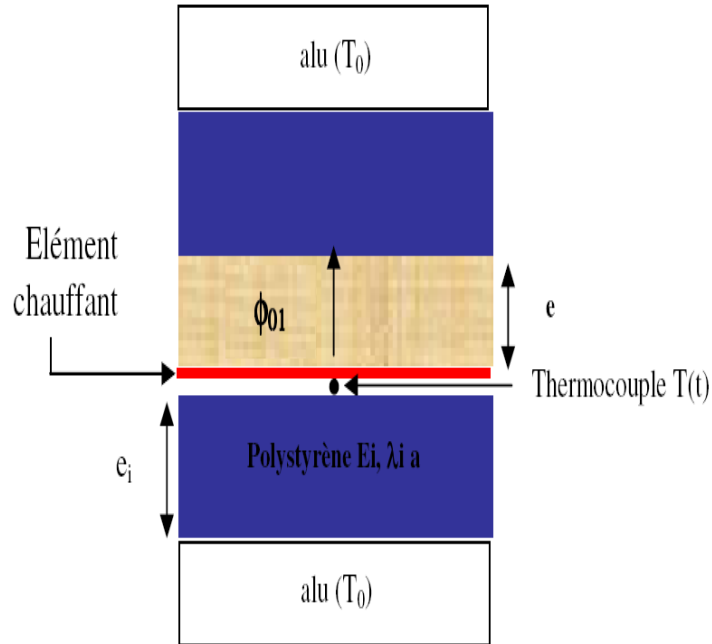


Figure 3: Asymmetric Hot Plan.

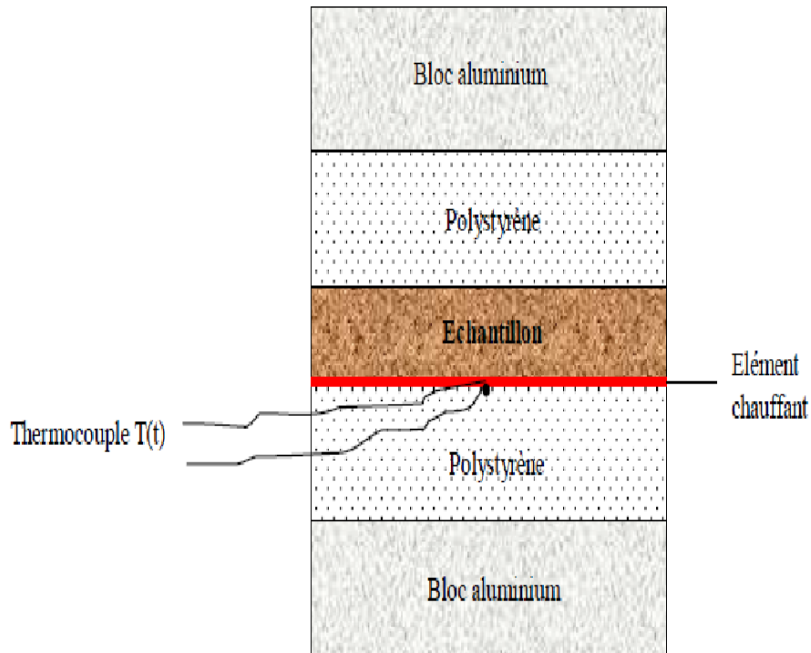


Figure 4:- Simplified Hot Plan Model.

An experimental study of the effusivity and thermal conductivity was mainly conducted using the method of the asymmetric hot plan in a transitory regime. Figure 3, shows the asymmetric experimental device. A plan heating device sharing the same section ($100 \times 100 \times 0.02 \text{ mm}^3$) with the sample is placed under it. K-type thermocouple comprising two cords of 0.005 mm diameter is placed at the underside of the heating device. The sample is placed between a 40 mm thick two blocks of extruded polystyrene set between two 40 mm thick aluminum blocks. A heat flow is sent from the heating device. The temperature evolution $T(t)$ is recorded at every each 0.1 s . The presence of the thermocouple does not increase the contact resistance between the heating device and the polystyrene.

Since polystyrene is an insulating material, this thermal resistance will be marginal. The system is modeled with the unidirectional transfer hypothesis (1D) at the center of the heating device and the sample during the measurement. This hypothesis is checked with 3D simulation using the COMSOL and residues analysis: the difference between the temperature provided by the theoretical model $T_{mod}(t)$ and that provided by the experience $T_{exp}(t)$, to determine the time t_{max} at which the unidirectional hypothesis (1D) is checked. Given the very low value of the heat flow reaching the aluminum blocks through the polystyrene and their high capacity, the temperature is assumed to be equal and constant. By applying the quadrupole formalism [17] on the device shown in Figure 3 & 4, and by using the temperature of the side before the sample $T_1(t)$:

$$\begin{bmatrix} \theta_1 \\ \Phi_1 \end{bmatrix} = \begin{bmatrix} 1 & 0 \\ C_s p & 1 \end{bmatrix} \begin{bmatrix} 1 & Rc_1 \\ 0 & 1 \end{bmatrix} \begin{bmatrix} A_e & B_e \\ C_e & D_e \end{bmatrix} \begin{bmatrix} A_i & B_i \\ C_i & D_i \end{bmatrix} \begin{bmatrix} 0 \\ \Phi_1' \end{bmatrix} = \begin{bmatrix} A & B \\ C & D \end{bmatrix} \begin{bmatrix} 0 \\ \Phi_1' \end{bmatrix} \quad (01)$$

$$C_s = \rho_s c_s e_s$$

$$\begin{bmatrix} A_e & B_e \\ C_e & D_e \end{bmatrix} = \begin{bmatrix} ch(qe) & \frac{sh(qe)}{\lambda q S} \\ \lambda q S sh(qe) & ch(qe) \end{bmatrix}, \begin{bmatrix} A_i & B_i \\ C_i & D_i \end{bmatrix} = \begin{bmatrix} ch(q_i e_i) & \frac{sh(q_i e_i)}{\lambda q_i S} \\ \lambda q_i S sh(q_i e_i) & ch(q_i e_i) \end{bmatrix} \text{ with}$$

$$q = \sqrt{\frac{P}{a}} \quad \text{et} \quad q_i = \sqrt{\frac{P}{a_i}}$$

The formula (01) leads to the following formula (02):

$$\begin{bmatrix} \theta_1 \\ \Phi_1 \end{bmatrix} = \begin{bmatrix} 1 & 0 \\ C_s p & 1 \end{bmatrix} \begin{bmatrix} 1 & Rc_1 \\ 0 & 1 \end{bmatrix} \begin{bmatrix} ch(qe) & \frac{sh(qe)}{\lambda q S} \\ \lambda q S sh(qe) & ch(qe) \end{bmatrix} \begin{bmatrix} ch(q_i e_i) & \frac{sh(q_i e_i)}{\lambda q_i S} \\ \lambda q_i S sh(q_i e_i) & ch(q_i e_i) \end{bmatrix} \begin{bmatrix} 0 \\ \Phi_1' \end{bmatrix} = \begin{bmatrix} A & B \\ C & D \end{bmatrix} \begin{bmatrix} 0 \\ \Phi_1' \end{bmatrix} \quad (02)$$

By developing the previous matrix product (01), then we get Φ_1 :

$$\Phi_1 = \theta_1 \frac{D}{B} \quad (03). \text{ Concerning the (polystyrene) insulator, we have } \begin{bmatrix} \theta_1 \\ \Phi_2 \end{bmatrix} = \begin{bmatrix} A_i & B_i \\ C_i & D_i \end{bmatrix} \begin{bmatrix} 0 \\ \Phi_2' \end{bmatrix} \quad (04)$$

by developing the previous matrix product, we have $\Phi_2 : \Phi_2 = \theta_1 \frac{D_i}{B_i}$ with $\Phi_0 = \Phi_1 + \Phi_2 = \frac{\phi_0}{S}$.

$$\text{So } \Phi_0 = \theta_1 \left(\frac{D}{B} + \frac{D_i}{B_i} \right) \text{ and then we draw the value of } \theta_1 \text{ using the relation } \theta_i = \frac{\phi_0}{P} \left(\frac{1}{\frac{D}{B} + \frac{D_i}{B_i}} \right) \quad (05).$$

With the inverse transformed, the relation (5) enables to get.

$$T_1(t) = L^{-1} \left(\frac{\phi_0}{P} \times \frac{1}{\left(\frac{D}{B} + \frac{D_i}{B_i} \right)} \right) \quad (06)$$

For the whole time, we used the unidirectional hypothesis (1D). Temperature at the center of the heating device in the Laplace area becomes:

$$\theta_s(0,0,p) = \frac{\Phi S}{2p} \frac{1 + R_c ES \sqrt{P}}{m_s c_s p + [R_c m_s c_s p + 1] ES \sqrt{P}} \quad (07) \text{ and after inversion with longer time we have :}$$

$$T_s(0,0,t) = \Phi \left[R_c - \frac{m_s c_s}{E^2 S^2} \right] + \frac{2\Phi \sqrt{t}}{ES \sqrt{\pi}} \quad (08)$$

The principle of the method is to determine the value of the effusivity E, the thermal conductivity λ of the sample and the contact resistance R_c that minimize the Mean Squared Error of the sum

$$\psi = \sum_{j=0}^N \left[\Delta T_{\text{exp}(t_j)} - T_{\text{mod}(t_j)} \right]^2 \quad (9) \text{ between the theoretical curve } T_{\text{cmod}(t)} = T_{\text{cmod}}(0,t) \text{ and the}$$

experimental curve $\Delta T_{\text{cexp}} = T_{\text{cexp}}(0,t) - T_{\text{cexp}}(e,t)$ (10) in the Levenberg-Marquardt-like algorithm **program**

[18]. θ_1 is the Laplace temperature transformed $T_1(t)$, Φ_1 is Laplace transformed of the heat flow from the probe toward the sample above. Φ_2 is Laplace transformed of the heat flow from the probe to the insulator (polystyrene) located at the bottom. Φ_0 is the sum of Laplace transformed of the total flux released by the probe to the sample (on top) and to the insulator (polystyrene) underneath. $C_s = \rho_s e_s c_s$ is the heat capacity per unit area of the probe. R_c is the contact resistance between the sample and the probe. e_i and e are the thicknesses of the insulator and the sample respectively. a_i is the thermal diffusivity of the polystyrene. Figure 5 shows the theoretical and experimental model.

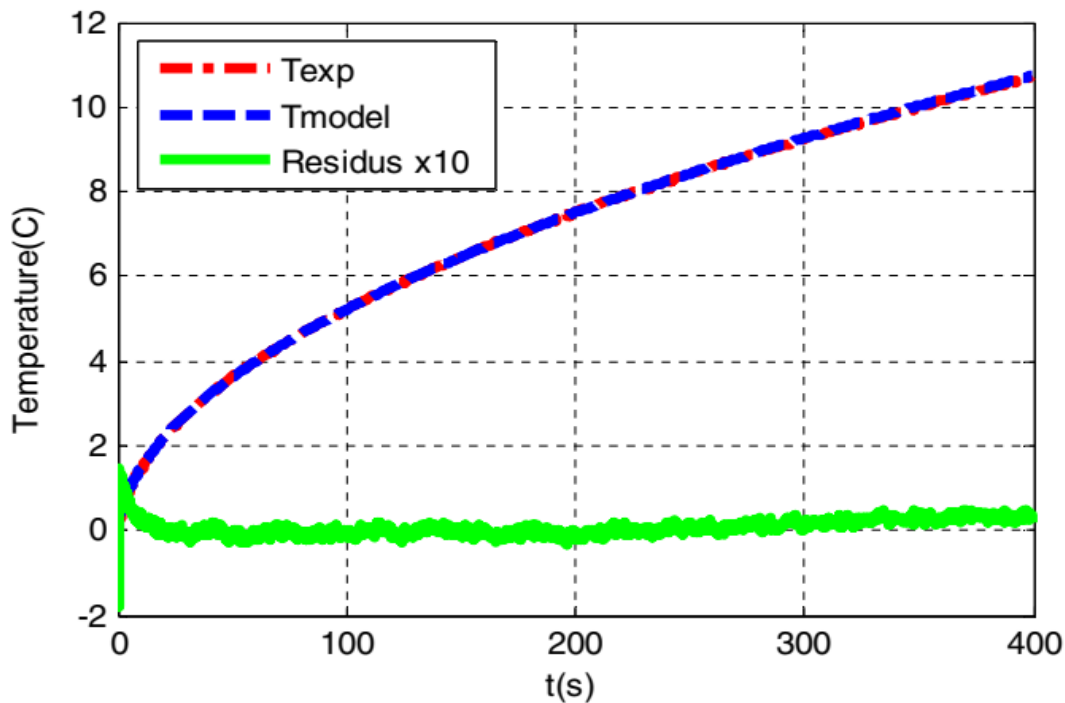


Figure 5:- Theoretical and experimental model.

Mechanical method

To build a house, it is necessary to know the response of the house to compressive and tensile forces. Compressive strength is measured by applying a force to the axis of a specimen placed between the plates of a press. This force is increased until the specimen breaks.

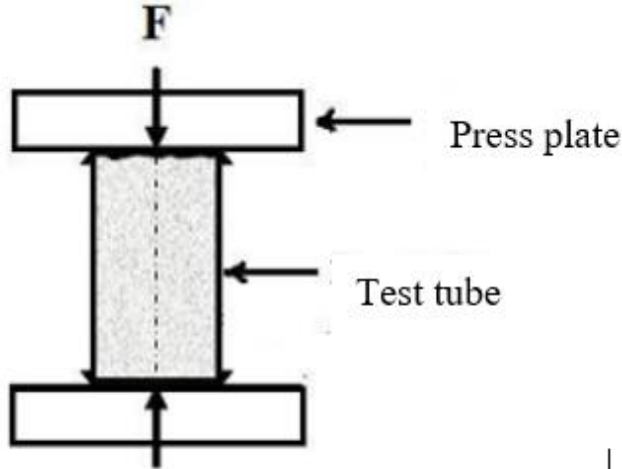


Figure 6:- Method of measuring compressive strength [21].

The compressive strength R_c , expressed in MPa, is given by the following relationship,

$$R_c = \frac{F}{S} \quad (11)$$

where F is the maximum value of the applied force in newtons (N) and S is the cross-sectional area of the specimen in mm^2 .

Results And Analysis:-

X-ray diffraction (XRD) of laterite

The equipment used is a diffractometer model X'PERT Pro MPD PANALYTICAL available at the Faculty of Sciences of Tunis, El Manar University. The laterite XRD results are presented in Figure 7.

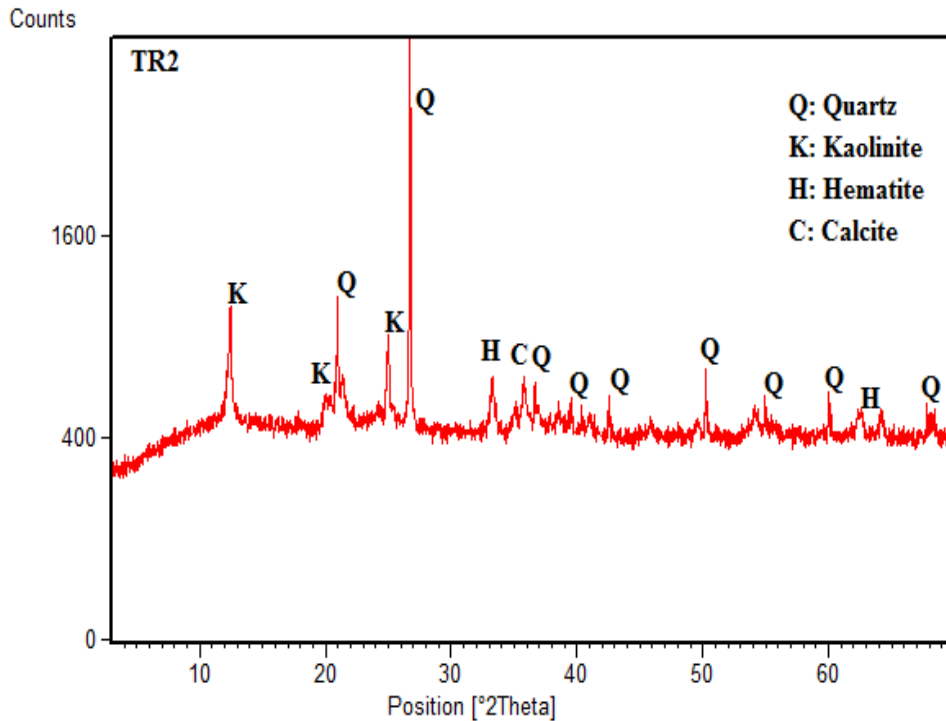


Figure 7:- X-ray diffractogram of laterite powders.

The XRD results show that our laterite consists of quartz (Q), kaolinite (K), hematite (H) and calcite.

Infrared spectroscopy (IR)

In the context of our study, the infrared spectrum of laterite presented in the following figure is obtained using a Nicolet 6700 FT instrument, over a recording range of 400 cm^{-1} to 4000 cm^{-1} in the mid-infrared region.

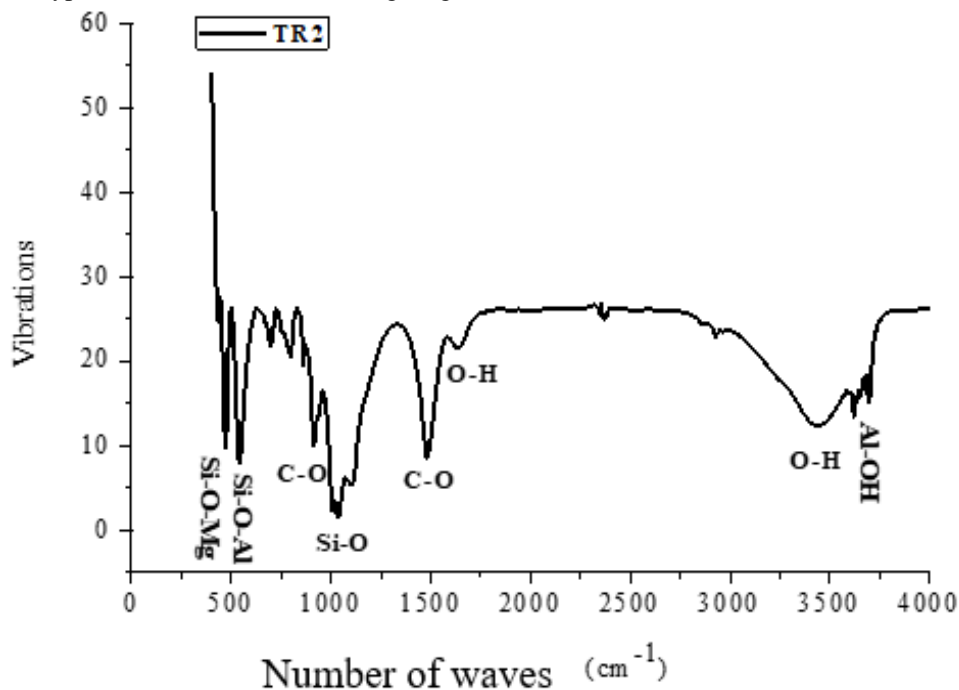


Figure 8:- IR spectrum of laterite.

The spectrum shows two essential groups: the OH and H₂O groups (bands of 1640 cm^{-1} and 3456 cm^{-1}) characterising deformation and elongation vibrations respectively; and the Si-O group (broad, intense band centred at around 1027 cm^{-1}) corresponding to the bond valence vibration in clay minerals. The relatively broad absorption band located around 3500 cm^{-1} is related to phyllosilicates such as kaolinite or illite. The absorption band around 1640 cm^{-1} may be due to the presence of interfoliar water. Overall, the IR spectrum confirms the information provided by the X-ray diffraction.

Elemental chemical analysis of laterite

The chemical composition of the laterite is presented in the following table.

Table 1:- Chemical composition of laterite (%).

Sample	SiO ₂	Al ₂ O ₃	Fe ₂ O ₃	MnO	MgO	CaO	Na ₂ O	K ₂ O	TiO ₂	P ₂ O ₅
Laterite	23.00	22.77	33.67	< L.D.	0.13	0.16	0.03	0.11	1.32	1.63

The results show that the most abundant oxides in our sample are SiO₂, Al₂O₃ and Fe₂O₃ while K₂O, CaO, MgO, Na₂O, TiO₂ and P₂O₅ are present only in small quantities.

The results in the previous table indicate that laterite has a high Fe₂O₃ content, which gives laterite bricks a reddish colour.

Differential thermal analysis (DTA)

In the context of our work, differential thermal analysis (DTA) of laterite in the raw state was carried out using the Setsys Evolution 1750 SETARAM. The analyses were carried out in dry air with a heating rate of $20^\circ\text{C}/\text{min}$ up to the desired maximum temperature (1200°C) without a step and cooling at the same. The ATD thermogram of laterite shows an endothermic peak at around 500°C corresponding to the dehydroxylation of clay minerals (kaolinite). This is followed by an exothermic peak at around 1000°C and another at around 1200°C which correspond to the structural reorganisation of the metakaolinite.

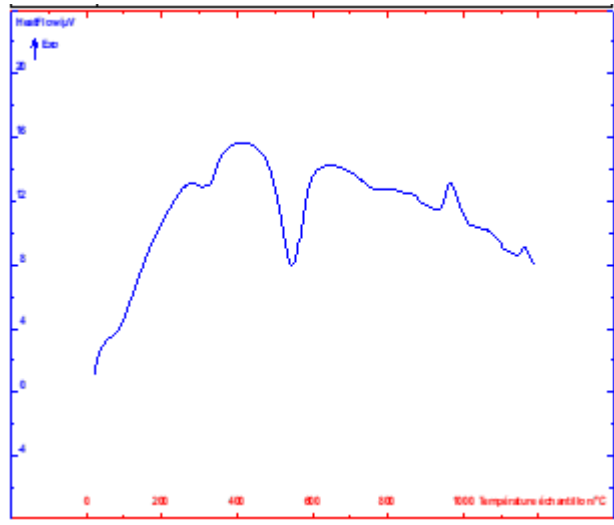


Figure 9:- ATD curve of laterite at 1200°C.

The ATD thermogram of laterite shows an endothermic peak at around 500°C corresponding to the dehydroxylation of clay minerals (kaolinite). This is followed by an exothermic peak at around 1000°C and another at around 1200°C which correspond to the structural reorganisation of the metakaolinite.

SEM microscopic observations

The microstructure of our sample was observed and analysed using a JSM-5400 scanning electron microscope (SEM). Figure 9 shows the SEM result obtained.

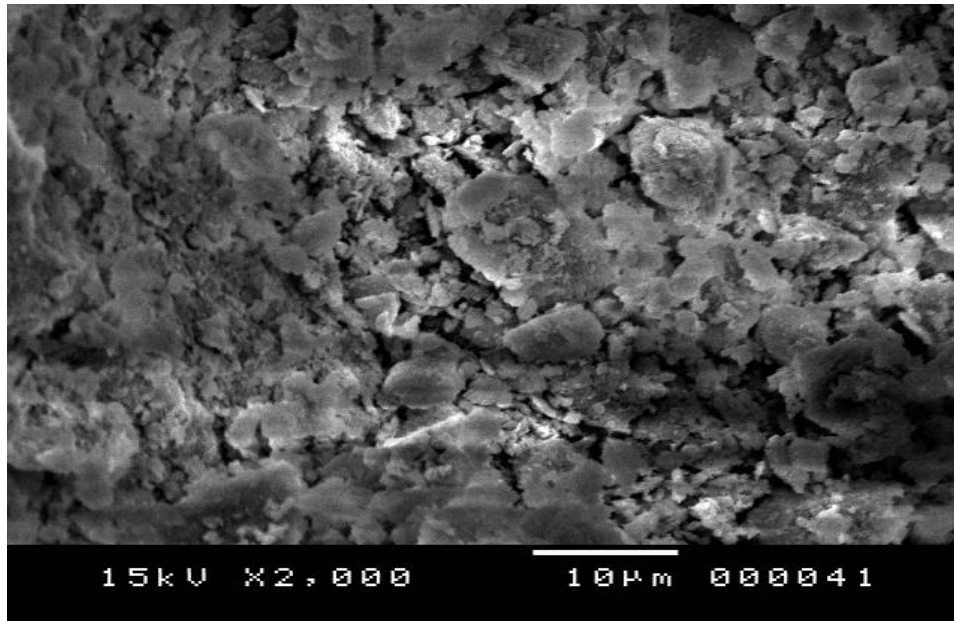


Figure 10:- SEM image of laterite.

Microscopic observation of our laterite shows that the texture is relatively compact, formed by several superimposed flat sheets with turbostratic disorder (random combination of rotations and translations). We observe the presence of quartz in the material. Some pores and microcracks are also present.

The laterite sample has an open texture with no preferential arrangement of layers. The random orientation of the laterite shows voids in the structure of the sample, and subsequently the appearance of a network of discontinuities.

Thermal results

Table 2:- Thermophysical properties of laterite.

Sample Number	$E(J / m.K.s^{\frac{1}{2}})$	$\frac{\Delta E}{E}(\%)$	$\lambda(W / m.K)$	$\frac{\Delta \lambda}{\lambda}(\%)$	$c(J / Kg.K)$	$\frac{\Delta c}{c}(\%)$
1st	798.746	0.069	0.375	0.188	170.32	0.124
2nd	752.77	0.066	0.366	0.177	1548.25	0.120
3rd	795.517	0.075	0.399	0.1812	1586.08	0.012
Mean	782.344	0.070	0.380	0.182	1611.88	0.085

The moisture content is determined according to NF P94-050. Lateritic soils easily absorb water (water of imbibition) at the surface of lateritic minerals. Indeed, this water disappears when drying at the temperature of 105°C Taha Ashour et al (2015) [19]. Moisture content quantifies the total amount of water contained in a material and provides information on its hydration status. It is expressed as a percentage of the mass of dry matter. The following relationship can be used to estimate the moisture content.

$$\varpi(\%) = \frac{(M_1 - M_2)}{M_1} \times 100$$

ϖ = moisture content

M_1 = The mass of the sample before steaming

M_2 = The mass of the sample after steaming at 105 °C for 24hours

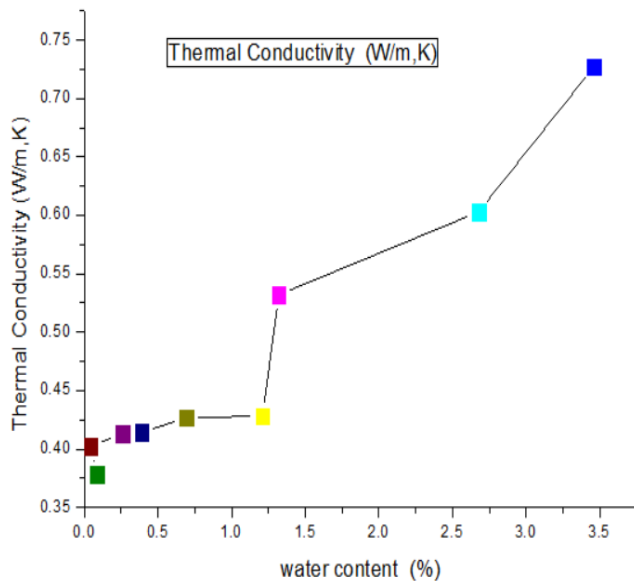


Figure 12: Thermal conductivity of Laterite as a function of water content

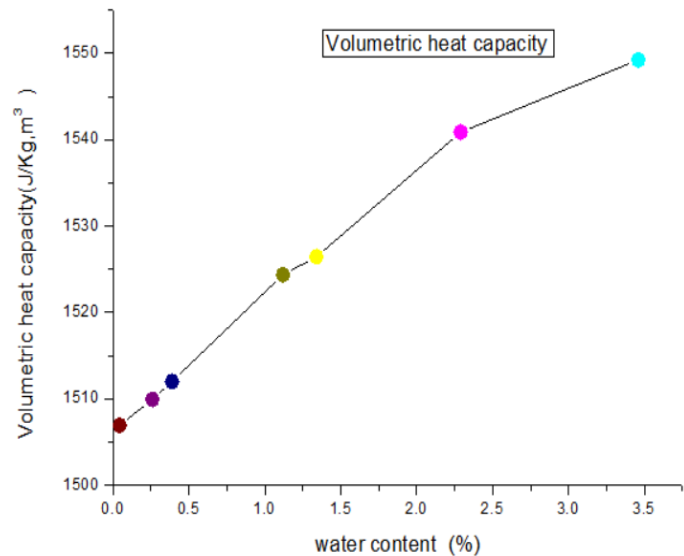


Figure 11: Volumetric heat capacity of Laterite as a function of water content

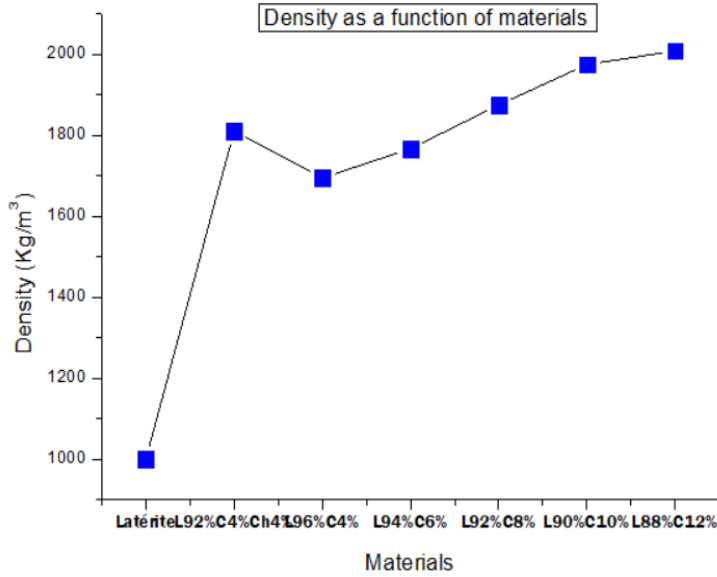


Figure 13:- Density as a function of materials.

The density of laterite increases when combined with 4% lime and 4% cement. The density of laterite when combined with 4% cement increases by 69.61%. It increases from 76.85%; 87.72%; 97.64% and 101.6% when 6%; 8%; 10% and 12% cement is added respectively.

Table 3:- Laterite92%+4% Cement+4% Lime.

Materials	$E(J/m.K.S^{1/2})$	$\frac{\Delta E}{E}(\%)$	$\lambda(W/m.K)$	$\frac{\Delta \lambda}{\lambda}(\%)$	$c(J/Kg.K)$	$\frac{\Delta c}{c}(\%)$
La92%C4%L4%	975.930	0.016	0.509	0.367	1033.812	0.399
	982.653	0.021	0.513	0.232	1038.109	0.274
	976.919	0.019	0.572	0.148	921.812	0.186
Average	978.500	0.018	0.531	0.249	997.911	0.286

The density of this material is: $\rho_{\text{Laterite92\%+4\%Cement+4\% Lime}} = 1810(Kg / m^3)$

Table 4:- Laterite96%+4% Cement.

Materials	$E(J/m.K.S^{1/2})$	$\frac{\Delta E}{E}(\%)$	$\lambda(W/m.K)$	$\frac{\Delta \lambda}{\lambda}(\%)$	$c(J/Kg.K)$	$\frac{\Delta c}{c}(\%)$
Latetrite96%+	1234.892	0.016	0.599	0.174	1502.466	0.206
4% Cement	1025.431	0.019	0.518	0.166	1198.002	0.204
	1020.939	0.017	0.509	0.160	1208.524	0.194
Average	1093.754	0.017	0.542	0.166	1302.997	0.201

The density of this material is: $\rho_{\text{Laterite96\%+Cement4\%}} = 1694,44(Kg / m^3)$

Table 5:- Laterite94%+6% Cement.

Materials	$E(J/m.K.S^{1/2})$	$\frac{\Delta E}{E}(\%)$	$\lambda(W/m.K)$	$\frac{\Delta \lambda}{\lambda}(\%)$	$c(J/Kg.K)$	$\frac{\Delta c}{c}(\%)$
	1022.706	0.020	0.547	0.259	1082.248	0.299
Laterite94%+6% Cement	986.413	0.023	0.589	0.219	935.007	0.265
	994.984	0.017	0.585	0.132	957.831	0.166
Average	1001.368	0.020	0.573	0.203	991.695	0.243

The density of this material is: $\rho_{\text{Laterite 94\%+Cement6\%}} = 1766.8(Kg / m^3)$

Table 6:- Laterite 92%+8% Cement.

Materials	$E(J/m.K.S^{1/2})$	$\frac{\Delta E}{E}(\%)$	$\lambda(W/m.K)$	$\frac{\Delta \lambda}{\lambda}(\%)$	$c(J/Kg.K)$	$\frac{\Delta c}{c}(\%)$
Laterite92%+	958.82	0.025	0.600	0.181	816.620	0.231
8% Cement	967.118	0.021	0.616	0.209	809.638	0.251
	986.222	0.056	0.577	0.415	898.848	0.527
Average	970.640	0.159	0.597	0.255	841.702	0.336

The density of this material is: $\rho_{\text{Laterite 92\%+Cement8\%}} = 1875.37(Kg / m^3)$

Tableau 7:- Laterite 90%+10% Cement.

Materials	$E(J/m.K.S^{1/2})$	$\frac{\Delta E}{E}(\%)$	$\lambda(W/m.K)$	$\frac{\Delta \lambda}{\lambda}(\%)$	$c(J/Kg.K)$	$\frac{\Delta c}{c}(\%)$
Laterite90%+	981.609	0.027	0.675	0.189	722.959	0.216
10% Cement	971.976	0.032	0.729	0.194	656.332	0.226
	988.288	0.018	0.576	0.347	858.786	0.365
Average	980.624	0.026	0.660	0.243	746.025	0.269

The density of this material is: $\rho_{\text{Laterite 90\%+Cement10\%}} = 1974,51(Kg / m^3)$

Table 8:- Laterite 88%+ 12% Cement.

Materials	$E(J/m.K.S^{1/2})$	$\frac{\Delta E}{E}(\%)$	$\lambda(W/m.K)$	$\frac{\Delta \lambda}{\lambda}(\%)$	$c(J/Kg.K)$	$\frac{\Delta c}{c}(\%)$
Laterite 88%+	1168.266	0.018	0.733	0.137	926.995	0.173
12% Cement	1150.179	0.019	0.730	0.136	902.206	0.174
	1136.960	0.015	0.669	0.152	961.990	0.182
Average	1151.801	0.017	0.710	0,141	930.397	0.145

The density of this material is: $\rho_{\text{Laterite 88\%+Cement12\%}} = 2008,64(Kg / m^3)$

Recent work by Azakine S et al. [20] on cement-stabilized earth blocks. The results of thermal properties of different formulations were measured by hot wire method. They obtained 0.59W/(m.K) with 4% cement content, then a value of 0.60W/(m.K) for 8% content, and finally a value of thermal conductivity of 0.66W/(m.K) and 0.72 W/(m.K) is obtained respectively for 10% and 12% cement content used as stabilizer. The results of his research are very close to those found by the L.E.A. asymmetric hot plane method with cement stabilised laterite with different formulations.

Analysis of mechanical results

The figure below shows the mechanical behaviour of laterite combined with cement at rates varying from 0%, 4%, 6%, 8% and 10% cement in laterite.

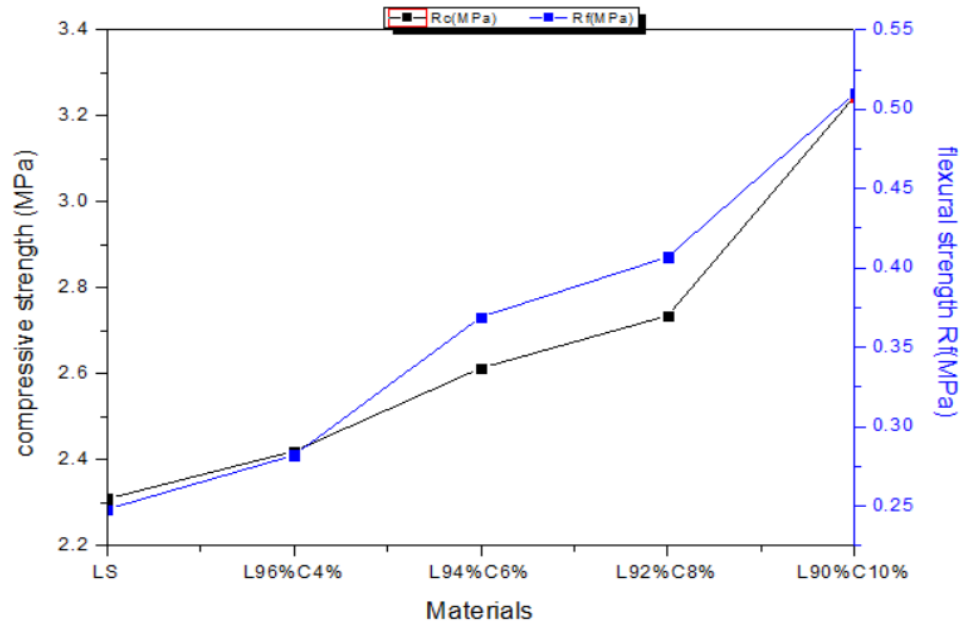


Figure 14:- Mechanical properties of laterite as a function of cement content.

Laterite without cement has a compressive strength of 2.309 MPa, this strength increases respectively by 4.80%; 13.16%; 18.45% and finally 42.92% when 4%; 6%; 8% and 10% cement is added to the laterite respectively. The flexural strength changes with the cement content of the mix, from 0.24 MPa for simple laterite to 0.510 MPa when 10% cement is added to the laterite. These results show that laterite bricks are poor materials in accordance with flexural strength.

Conclusion:-

The thermophysical parameters of laterite evolve rapidly as a function of the water content and also as a function of the cement content in the mix. For laterite with a diameter less than or equal to 1.25mm, the thermal conductivity is 0.388 W/m.K at a water content close to 0%, this thermal conductivity increases by 87.37% for a water content of 3.46%. This value increases by 82.98% when 12% of the cement mass is added to the mix. The compressive and flexural strength changes with the amount of cement in the mix. The compressive and flexural strength increases by 47.82% and 112.5% respectively when the laterite is stabilised with 10% cement.

Acknowledgements:-

The authors thank ISP at Uppsala University, Sweden, for supporting the BUF01 project.

References:-

- [1] Adriana Bel'enCostantini Romero, Franco Matias Francisca Ignacio Giomi: Hygrothermal properties of soil-cement construction materials: Construction and Building Materials 313 (2021) 125518.
- [2] Fezzioui N et Benyamine M. Maison à patio: Réponses aux exigences sociologiques culturelles et thermiques. Conférence internationale : Medina. Tissu urbain à sauvegarder. Tlemcen. 13-14 Mai 2008.
- [3] Les systèmes de ventilation et de climatisation. Institut de l'Energie et de l'Environnement de la Francophonie (IEPF). Fiche Technique PRISME n°2; 2001.
- [4] Pape Moussa Touré, Younouss Dièye, Prince momar Gueye, Vincent Sambou, Seckou Bodian and Sumaila Tigampo: Experimental determination of time lag and decrement factor: Case studies in Constructions Materials 11(2019)e00298.
- [5] Kowa K. Eric, Jean Claude Damfeu, Pettang J. Ursulala, Joel Ducourneau, Paul Wofo, Chispin Pettang: Thermophysical and Mechanical Characterization of Poto-Poto Compressed Blocks for Use as Fill Material : Materials Sciences and Applications, 2021, 12, 437-459. <https://www.scirp.org/journal/msa>.
- [6] Adriana Belén Costantini Romero, Franco Matias Francisca, Hygrothermal properties of soil-cement construction materials: Construction and Building Materials, Volume 313, 27 December 2021, 125518.

- [7] Y. Millogo, J.C. Morel, K. Traoré, R. Ouedraogo, Microstructure, geotechnical and mechanical characteristics of quicklime-lateritic gravels mixtures used in road construction. *Constr. Build. Mater.* 2012; 26 (1), 663-669.
- [8] N. Laaroussi; A. Cherki, M.Garoum, A. Khabbazi, A. Feiz: Thermal properties of a sample prepared using mixtures of clay bricks. *Energy Procedia* 42 (2013) 337-346.
- [9] N. Laaroussi. G.Lauriat; M.Garoum; A. Cherki, Y.Jannot: Measurement of thermal properties of brick materials based on clay mixtures. *Construction and Building Materials* 70 (2014) 351-361.
- [10] P. Meukam and al, 2004 'Thermophysical characteristics of economical building materials,' *Construction and building materials* 18(2004)437-443.
- [11] Imbga B. Kossi, Kieno P. Florent, Sambou Vincent, Ouedraogo Emmanuel, Gouba Daniel and Toure P. Moussa, Study of the Thermal and Mechanical Performance of Laterite Blocks Mixed with Néré Pod for the Thermal Insulation of Buildings, *Physical Science International Journal.* 2016; 11(2), 1-10.
- [12] J.C. Damfeu, P. Meukam, Y. Jannot: Modeling and estimation of the thermal properties of clusters aggregates for construction materials: The case of clusters aggregates of lateritic soil, sand and pouzzolan *International Journal of Heat and Mass Transfer* 102 (2016) 407-416.
- [13] Harouna Bal, Yves Jannot, Nathan Quenette, Alain Chenu, Salif Gaye: Water content dependence of the porosity, density and thermal capacity of laterite based bricks with millet waste additive, *Construction and Building Materials* 31 (2012) 144 – 150.
- [14] Colbert Babé, Dieudonné Kaoga Kidmo, Ahmat Tom, Rachel Raïssa Ngono Mvondoc, Raphaël Belinga Essama Boum, Noël Djongyang: Thermomechanical characterization and durability of adobes reinforced with millet waste fibers (sorghum bicolor). *Case Studies in Construction Materials* 13 (2020) e00422.
- [15] Séckou Bodian, Mactar Faye, Ndeye Awa Sene, Vincent Sambou, Oualid Limam, Ababacar Thiam; Thermo-mechanical behavior of unfired bricks and fired bricks made from a mixture of clay soil and laterite, *Journal of Building Engineering* 18 (2018) 172-179.
- [16] Pape Moussa Toure, Vincent Sambou, Mactar Faye, Ababacar Thiam; Thermal and mechanical characterization of stabilized earth bricks. *Energy Procedia* 139 (2017) 676-681.
- [17] F. R. de Hoog, J. H. Knight, and A. N. Stokes. An Improved method for numerical inversion of Laplace Transforms. *Society of Industrial and Applied Mathematics.* 1982; 3(3); 357-366.
- [18] De Hoog FR: An Improved method for numerical inversion of Laplace Transforms. *Society of Industrial and Applied Mathematics;* 3(3); 357-366 (1982).
- [19] Taha Ashour, Azra Korjenic, Sinan Korjenic, Wei Wu: Thermal conductivity of unfired earth bricks reinforced by agricultural wastes with cement and gypsum, *Energy and Buildings* 104 (2015) 139 – 146
- [20] Azakine Sindanne S, Ntamack GE, Lemanle Sanga RP, Moubeke CA , Kelmamo Sallaboui ES, Bouabid H, Mansouri K, D'Ouazzane SC: Thermophysical characterization of earth blocks stabilized by cement, sawdust and lime ; *J. Build. Mater. Struct.* (2014) 1: 58-64.
- [21] M. BOUKAR, «Détermination des caractéristiques thermophysiques des matériaux locaux destinés à l'isolation des enceintes de conservation de froid et à celle des bâtiments», Thèse de Doctorat d'Etat és-Sciences, Université Cheikh Anta Diop de Dakar, 2013.